Biochemical Pharmacology 78 (2009) 617–624

Contents lists available at ScienceDirect

Biochemical Pharmacology

journal homepage: www.elsevier.com/locate/biochempharm

Effects of CYP2D6 status on harmaline metabolism, pharmacokinetics and pharmacodynamics, and a pharmacogenetics-based pharmacokinetic model

Chao Wu, Xi-Ling Jiang, Hong-Wu Shen, Ai-Ming Yu *

Department of Pharmaceutical Sciences, School of Pharmacy and Pharmaceutical Sciences, University at Buffalo, The State University of New York, Buffalo, NY 14260-1200, USA

ARTICLE INFO

Article history:
Received 9 March 2009
Accepted 7 May 2009

Keywords:
CYP2D6
Pharmacogenetics
Harmaline
Pharmacokinetics
Transgenic mouse

ABSTRACT

Harmaline is a β-carboline alkaloid showing neuroprotective and neurotoxic properties. Our recent studies have revealed an important role for cytochrome P450 2D6 (CYP2D6) in harmaline *O*-demethylation. This study, therefore, aimed to delineate the effects of CYP2D6 phenotype/genotype on harmaline metabolism, pharmacokinetics (PK) and pharmacodynamics (PD), and to develop a pharmacogenetics mechanism-based compartmental PK model. In vitro kinetic studies on metabolite formation in human CYP2D6 extensive metabolizer (EM) and poor metabolizer (PM) hepatocytes indicated that harmaline *O*-demethylase activity (V_{max}/K_m) was about 9-fold higher in EM hepatocytes. Substrate depletion showed mono-exponential decay trait, and estimated in vitro harmaline clearance (CL_{int}, μL/min/10^6 cells) was significantly lower in PM hepatocytes (28.5) than EM hepatocytes (71.1). In vivo studies in *CYP2D6*-humanized and wild-type mouse models showed that wild-type mice were subjected to higher and longer exposure to harmaline (5 and 15 mg/kg; i.v. and i.p.), and more severe hypothermic responses. The PK/PD data were nicely described by our pharmacogenetics-based PK model involving the clearance of drug by CYP2D6 (CL_{CYP2D6}) and other mechanisms (CL_{other}), and an indirect response PD model, respectively. Wild-type mice were also more sensitive to harmaline in marble-burying tests, as manifested by significantly lower ED_{50} and steeper Hill slope. These findings suggest that distinct CYP2D6 status may cause considerable variations in harmaline metabolism, PK and PD. In addition, the pharmacogenetics-based PK model may be extended to define PK difference caused by other polymorphic drug-metabolizing enzyme in different populations.

1. Introduction

Cytochrome P450 2D6 (CYP2D6) is one of the most important polymorphic phase I drug-metabolizing enzymes that is involved in the biotransformation of 20–30% of marketed drugs and some endogenous substrates [1,2]. Individuals with impaired or deficient CYP2D6 activity could be more sensitive to CYP2D6-metabolized drugs, which is likely dependent on the fraction of CYP2D6-mediated metabolism in total drug clearance and the range between therapeutic and toxic doses of the drug. CYP2D6 also metabolizes a variety of drugs of abuse such as amphetamines [3–6], indoleamines [7–9] and many other designer drugs [10,11]. Delineation of the impact of CYP2D6 on the metabolism, pharmacokinetics (PK) and pharmacodynamics (PD) of these substances would provide increased understanding of individual vulnerability to and/or protection from illicit drugs of abuse [12].

Harmaline, 3,4-dihydro-7-methoxy-1-methyl-β-carboline, is a major form of alkaloid in the seeds of *Peganum harmala* (Syria rue) that has been used in traditional medicine and for recreational purpose [13]. Harmaline is also a typical psychotropic ingredient in the recreational beverage *Ayahuasca*, which shows potential in treating many psychiatric disorders [14], whereas the therapeutic potential and medical uses are hampered by many safety issues including abuse liability. Harmaline readily modulates the levels of amine neurotransmitters via inhibition of monoamine oxidase. It may directly bind to specific receptors including 5-HT, benzodiazepine and imidazoline receptors. With diverse biochemical properties, harmaline has shown neuroprotective, anxiolytic, antinociceptive, antioxidant and vasorelaxant properties in animal models [15–19]. On the other hand, harmaline alone or along with other tryptamine substances may result in severe or even fatal toxicities in animals [20–22] and in humans [23–25]. Of particular note, harmaline acts on the olivo-cerebellar system, causes rhythmic activity, and leads to postural tremors in animal models. Harmaline-induced tremor has many similar characteristics as essential tremor, a common movement disorders in humans.

Abbreviations: CYP2D6, Cytochrome P450 2D6; PK, pharmacokinetics; PD, pharmacodynamics; EM, extensive metabolizer; PM, poor metabolizer; Tg-*CYP2D6*, *CYP2D6*-humanized; IDR, indirect response; HPLC, high performance liquid chromatography; LC-MS/MS, liquid chromatography tandem mass spectrometry.

* Corresponding author. Tel.: +1 716 645 2842; fax: +1 716 645 3893.
E-mail address: aimingyu@buffalo.edu (A.-M. Yu).

0006-2952/$ – see front matter © 2009 Elsevier Inc. All rights reserved.
doi:10.1016/j.bcp.2009.05.011

Therefore, harmaline tremor has been widely used as a model to understand the pathogenesis of essential tremor and to develop therapeutic agents for generalized tremor [21,22,26].

Following an acute administration to rats, harmaline is rapidly distributed into different organs and mainly metabolized via *O*-demethylation [27]. Recently we have shown that harmaline *O*-demethylation is primarily catalyzed by cytochrome P450 2D6 (CYP2D6) and CYP1A2 in human liver microsomes [28]. This study, therefore, aimed to (1) define the effects of CYP2D6 status on harmaline metabolism, pharmacokinetics and pharmacodynamics, and (2) use harmaline as a model drug to develop pharmacogenetics-based PK compartmental model to provide increased understanding of the PK difference caused by CYP2D6 metabolism.

2. Materials and methods

2.1. Chemicals and materials

Harmaline hydrochloride dihydrate, harmalol hydrochloride dihydrate and β-glucuronidase were purchased from Sigma–Aldrich (St. Louis, MO). Cryopreserved human hepatocytes, *InVitro*GRO HT Medium, KHB buffer and Torpedo Antibiotic Mix were purchased from Celsis (Chicago, IL) or BD Biosciences (San Jose, CA). The lot numbers of CYP2D6 PM hepatocyte samples were VTA (dextromethorphan *O*-demethylase activity, 1 pmol/min/10^6 cells; CYP2D6 genotype, **3/*4*), ETR (1 pmol/min/10^6 cells; **4/*4*), PFM (1 pmol/min/10^6 cells; **1/*7*), and HH183 (bufuralol 1′-hydroxylase activity, not detectable), and EM hepatocyte samples were GNG (17 pmol/min/10^6 cells; **1/*4*), KRM (36 pmol/min/10^6 cells; **1/*4*), KRJ (40 pmol/min/10^6 cells; **1/*4*), VEN (69 pmol/min/10^6 cells; **1/*1*), AGR (96 pmol/min/10^6 cells; genotyped not determined), and HH169 (bufuralol 1′-hydroxylase activity, 60 pmol/min/10^6 cells). Dulbecco's Modified Eagle's Medium (DMEM) was bought from Mediatech, Inc. (Manassas, VA). All other reagents or organic solvents used were either analytical or high performance liquid chromatography (HPLC) grade.

2.2. Animals

Age-matched (7–10 weeks old) male wild-type FVB/N and CYP2D6-humanized (Tg-*CYP2D6*) mice [29] weighing 25–32 g were used in the study. Animals were housed in an animal care facility maintained at 20 ± 2 °C on a 12 h light/dark cycle. Food and water were provided *ad libitum*. All animal procedures were approved by the Institutional Animal Care and Use Committee at University at Buffalo, The State University of New York.

2.3. Drug metabolism in human hepatocytes

Cryopreserved human hepatocytes were thawed in a 37 °C water bath, and suspended in pre-warmed suspension media (DMEM or *InVitro*GRO HT Medium supplemented with Torpedo Antibiotic Mix, 49/1, v/v). Cell suspension was mixed gently, centrifuged at 500 rpm for 5 min at 4 °C. After the supernatant was removed, cells were resuspended in incubation media, and cell viability was determined by the Trypan Blue exclusion test.

Reaction was initiated by mixing the same volume of drug solution (in KHB buffer) and resuspended hepatocytes, and the mixture was incubated at 37 °C, 5% carbon dioxide and saturating humidity. In metabolite production kinetic studies, incubations were conducted with 96-well plate, and all reactions were carried out in triplicate. Each well consisted of 0.25×10^6 cells/mL of hepatocytes and desired concentrations of harmaline (0.5–150 μM) in a total volume of 200 μL. Reaction mixtures were snap-frozen in liquid nitrogen after 30 min incubation. In substrate depletion kinetic studies, incubations were carried out using 6-well plate and all reactions were performed in duplicate. Each well consisted of 2 μM of harmaline and 0.5×10^6 cells/mL of hepatocytes in a total volume of 1.6 mL. Forty microliter of media were aliquoted at different time point (0, 15, 30, 45, 60 and 90 min) and snap-frozen in liquid nitrogen.

2.4. Pharmacokinetic studies

Adult male Tg-*CYP2D6* and wild-type mice were randomized to receive either 5 or 15 mg/kg of harmaline intravenously (i.v.) or intraperitoneally (i.p.). Blood samples were collected from retro-orbital plexus at different time points (0–120 min, $N = 3$ per time point) after drug administration. Serum was prepared with a serum separator (BD Biosciences, San Jose, CA), and stored at −80 °C until analysis.

2.5. Sample preparation and drug/metabolite quantification

Upon analyses, hepatocyte samples were thawed on ice, and cells were removed by centrifugation. Forty microliter of sample were digested with β-glucuronidase (80 U in 40 μL of 0.2% sodium chloride solution) in 0.2 M sodium acetate buffer (pH 4.75, 80 μL) at 37 °C for 3 h. The mixture was then deproteinized with 5 μL of ice-cold perchloric acid (70%) and centrifuged at 14,000 × *g* for 10 min. The supernatant was transferred into new vials and injected for HPLC analysis. Likewise, serum sample (40 μL) was digested with β-glucuronidase, and the mixture was processed by liquid–liquid extraction with 2 mL of methyl t-butyl ether/ethyl acetate (v/v, 1:2). The organic layer was transferred into new tubes, evaporated to dryness, reconstituted with 40 μL of 50% methanol containing 0.1% formic acid, and then analyzed by tandem mass spectrometry (MS/MS).

HPLC quantification of harmaline and harmalol in hepatocyte samples was performed as reported [28] on an Agilent 1100 series HPLC system consisting of the online vacuum degasser, quaternary pump, autosampler, thermostat controlled column compartment, fluorescence detector and diode-array detector. The calibration curve was linear from 0.2 to 500 pmol for both harmaline and harmalol. Assay accuracy was 95–110%, and intra-day and inter-day variations were both less than 10%.

The LC-MS/MS system used for the analyses of serum samples consisted of a Shimadzu prominence HPLC (Kyoto, Japan) coupled to an API 3000 turbo ionspray ionization triple-quadrupole mass spectrometer (Applied Biosystems, Foster City, CA). A Phenomenex phenyl–hexyl column (50 mm × 4.6 mm, 3 μm; Torrance, CA) was used for the analyses. A gradient elution was employed to separate the analytes, which included an initial 1-min isocratic elution with 75% of Buffer A (0.1% formic acid in water) and 25% of Buffer B (0.1% formic acid in methanol), an increase of Buffer B to 90% at 1.1 min and then elution with 90% of Buffer B for 3 min, followed by the initial condition from 4.1 min. The mass spectrometer was operated in positive mode with transitions m/z 215.2 → 174.2, 201.2 → 160.2, and 203.2 → 158.3 for harmaline, harmalol, and 5-methyl-*N*,*N*-dimethyltryptamine (internal standard), respectively. An online motorized six-port divert valve was used to introduce the LC eluent to the mass spectrometer over the period of 2.5–6 min for data acquisition, whereas eluent of 0–2.5 min was diverted to the waste. Calibration curve was linear from 12.3 to 27,000 nmol/L for harmaline, and linear from 37 to 27,000 nmol/L for harmalol, respectively. Assay accuracy was 91–106%, and intra-day and inter-day variations were both less than 10%.

2.6. Measurement of body temperature

After i.p. administration of harmaline (5 or 15 mg/kg) or vehicle control, mouse body temperature was monitored at different time

points (0, 5, 10, 15, 20, 30, 45, 60, 90 120, 150 and 180 min) using a High Precision Digital Thermometer with a microprobe (Barnstead International, Dubuque, IA) that was inserted about 1.5 cm into the rectum [30].

2.7. Marble-burying test

Thirty minutes after i.p. administration of harmaline (0–10 mg/kg) or drug vehicle, mouse was placed in a 28 cm × 17 cm × 16 cm transparent plastic cage with 5-cm layer of sawdust (Harlan Sani-Chips, Harlan-Teklad, Indianapolis, IN) on the floor and 20 glass marbles (1.5 cm diameter) distributed evenly against the wall of the cage. Mouse was removed from the cage after 30 min, and the number of marbles buried (at least 2/3 in the sawdust) was recorded and normalized with vehicle control.

2.8. Data analyses

All values were expressed as mean ± SD when experiments were carried out using different samples, or mean ± SEM when using the same sample. Enzyme kinetic parameters were estimated by non-linear regression using GraphPad Prism 5 (San Diego, CA). Specifically, metabolite formation data were fit to one-enzyme or two-enzyme Michaelis–Menten equation, and intrinsic clearance (CL_{int}) was calculated as V_{max}/K_m. Substrate depletion data were fit to mono-exponential decay model, $C_{(t)} = C_0 \cdot e^{-kt}$, where C_0 is the initial drug concentration in the incubation, and k is the terminal depletion rate constant. In vitro half-life ($T_{1/2}$) was calculated by dividing 0.693 by the rate constant. In vitro clearance (CL_{int}) was calculated by dividing initial dose (D_0) by the area under the concentration–time curve (AUC), and normalized with cell variability.

PK/PD modeling was conducted using WinNonLin (version 5.0, Pharsight, Mountain View, CA). Serum drug concentration data were first analyzed by non-compartmental model, essentially the same as described [31]. A pharmacogenetics-based PK model (Fig. 1) was then constructed to illustrate harmaline PK difference in Tg-*CYP2D6* and wild-type mice. The initial estimates were obtained from non-compartmental analysis. Parameters describing the pharmacogenetics-based PK model include the clearance contributed by CYP2D6-mediated metabolism (CL_{CYP2D6}) and clearance contributed by other elimination mechanisms (CL_{other}), volume of distribution of the central compartment (V_C) and peripheral compartment (V_T), absorption rate constant (K_a), distribution clearance between central and peripheral compartments (CL_D), and bioavailability (F). Note that harmaline is eliminated by CL_{CYP2D6} and CL_{other} in Tg-*CYP2D6* mice (or EMs), i.e., $CL = CL_{CYP2D6} + CL_{other}$, whereas the drug is eliminated by CL_{other} only in wild-type control mice (or PMs), i.e., $CL = CL_{other}$. In contrast, drug absorption (K_a) and distribution (CL_D) properties are the same in the two genotyped subjects. Once the pharmacogenetics-based PK model was finalized, the associated PK parameters were set as constants and linked to the PD model (Fig. 1), in which the time course of hypothermic response was sequentially analyzed by the basic indirect response (IDR) model IV [32]. Change of mouse body temperature (T) is due to heat production (k_{in}) and loss (k_{out}) nature of temperature control.

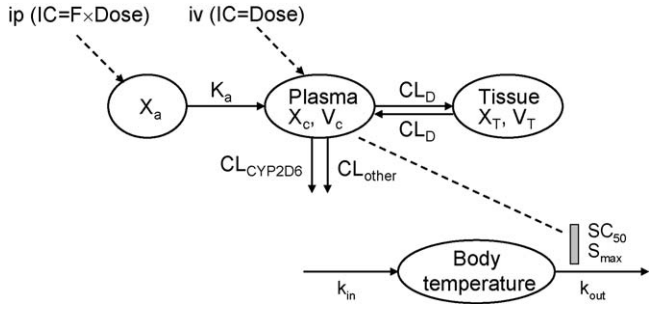

Fig. 1. Schematic representation of the PK/PD model consisting of a pharmacogenetics-based compartmental PK model of harmaline following i.p. and i.v. administration, and an indirect response pharmacodynamic model with stimulation of k_{out} (IDRIV) for harmaline-induced hypothermia following i.p. administrations. PK model: X_a, drug amount at the absorption site; K_a, absorption rate constant; F, bioavailability. X_C and X_T represent harmaline amount in central and peripheral compartment, respectively; V_C and V_T represent volume of distribution of harmaline in central and peripheral compartment, respectively; CL_{CYP2D6} and CL_{other} represent clearance of drug from central compartment contributed by CYP2D6-mediated metabolism and other elimination pathways, respectively; CL_D represents distribution clearance of harmaline between central and peripheral compartments. PD model, k_{in}, zero order rate constant of heat production; k_{out}, the first order rate constant of heat loss; S_{max}, the maximum fractional drug effect; SC_{50}, drug concentration required to produce 50% of the maximum effect. Of particular note, drug (e.g., harmaline) is eliminated by CL_{CYP2D6} and CL_{other} in Tg-*CYP2D6* mice (or EMs), i.e., $CL = CL_{CYP2D6} + CL_{other}$, whereas the drug is eliminated by CL_{other} only in wild-type control mice (or PMs), i.e., $CL = CL_{other}$.

The differential equations derived from the final PK/PD model (Fig. 1) were as follows:

$$\frac{dX_a}{dt} = -k_a \times X_a \quad (IC = F \times Dose) \tag{1}$$

$$\frac{dX_C}{dt} = k_a \times X_a - (CL_{CYP2D6} + CL_{other} + CL_D) \times \frac{X_C}{V_C} + CL_D \times \frac{X_T}{V_T} \quad (IC = 0) \tag{2}$$

$$\frac{dX_C}{dt} = k_a \times X_a - (CL_{other} + CL_D) \times \frac{X_C}{V_C} + CL_D \times \frac{X_T}{V_T} \quad (IC = 0) \tag{3}$$

$$\frac{dX_C}{dt} = -(CL_{CYP2D6} + CL_{other} + CL_D) \times \frac{X_C}{V_C} + CL_D \times \frac{X_T}{V_T} \quad (IC = Dose) \tag{4}$$

$$\frac{dX_C}{dt} = -(CL_{other} + CL_D) \times \frac{X_C}{V_C} + CL_D \times \frac{X_T}{V_T} \quad (IC = Dose) \tag{5}$$

$$\frac{dX_T}{dt} = CL_D \times \frac{X_C}{V_C} - CL_D \times \frac{X_T}{V_T} \quad (IC = 0) \tag{6}$$

$$\frac{dT}{dt} = k_{in} - k_{out} \times \left(1 + \frac{S_{max} \times C_c}{SC_{50} + C_c}\right) \times T \quad (IC = T_0) \tag{7}$$

Eqs. (1), (2) and (6) were used to fit the i.p. data, and (4) and (6) fit the i.v. data of Tg-*CYP2D6* mice, respectively. Likewise, Eqs. (1), (3) and (6) were used to fit the i.p. data, and (5) and (6) fit the i.v. data of wild-type mice, respectively. Eq. (7) was used to fit mouse body temperature data, where C_c is drug concentration in central compartment, S_{max} reflects the maximum fractional drug effect, SC_{50} is the drug concentration producing 50% of the maximum effect, and k_{in} can be defined as the initial condition of body temperature (T_0) times k_{out}. The appropriate PK/PD model was selected based on the goodness-of-fit criteria including coefficient variation of the estimates (CV%), R^2, Akaike's Information Criterion and Schwarz Criterion.

Mouse marble-burying data were fit to the empirical dose-response model (normalized response $= 100/(1 + 10^{((\log IC_{50} - \log Dose) \times Hill\ Slope)})$ (GraphPad Prism 5).

Depending on the number of groups and variances, data were analyzed by unpaired Student's t-test, one-way ANOVA analysis followed by Dunnett's test, or two-way ANOVA analysis (GraphPad Prism 5). Significant difference was considered if the probability was less than 0.05 ($P < 0.05$).

3. Results

3.1. Harmaline O-demethylase activity is much lower in human CYP2D6 PM hepatocytes

To delineate the effects of CYP2D6 status on harmaline metabolism, we first compared harmalol production between CYP2D6 EM and PM hepatocytes in vitro. Interestingly, all EM hepatocytes ($N = 5$) showed monophasic Michaelis–Menten enzyme kinetics, whereas PM hepatocytes ($N = 4$) exhibited biphasic kinetics (Fig. 2). Estimated enzyme efficiency (V_{max}/K_m, μL/min/10^6 cells) was about 9-fold lower in CYP2D6 PM hepatocytes (0.71 ± 0.44) than that in CYP2D6 EM hepatocytes (6.32 ± 2.35) (Table 1). The results suggest that PMs with CYP2D6 deficiency may have a lower capacity to catalyze harmaline *O*-demethylation metabolism.

3.2. Harmaline depletion is significantly slower in CYP2D6 PM hepatocytes

We then investigated the impact of CYP2D6 status on overall harmaline depletion in human hepatocytes. The data showed that harmaline depletion was significantly slower in CYP2D6 PM hepatocytes ($N = 4$) than EM hepatocytes ($N = 6$) (Fig. 3A). Consistently, harmalol levels were much higher in CYP2D6 EM hepatocytes (Fig. 3B). Kinetic parameters were estimated for harmaline depletion using mono-exponential decay model. Harmaline in vitro half-life ($T_{1/2}$, min) was much longer in CYP2D6 PM hepatocytes (111 ± 28) than EM hepatocytes (46.1 ± 15.8), which was consistent with a significantly lower in vitro intrinsic clearance (CL_{int}, μL/min/10^6 cells) in PM hepatocytes (28.5 ± 6.2) than that in EM hepatocytes (71.1 ± 23.1) (Table 2). The results suggest that CYP2D6 status could be an important factor controlling harmaline metabolic elimination.

3.3. Exposure to harmaline is much higher and longer in wild-type mice than Tg-CYP2D6 mice

We thus employed Tg-*CYP2D6* and wild-type mouse models to examine the effects of CYP2D6 status on harmaline PK. Serum harmaline concentration versus time courses were monitored (Fig. 4) in the two genotyped mice after administration of harmaline (5 and 15 mg/kg; i.v. and i.p.). Non-compartmental analyses of harmaline PK profiles showed that wild-type mice lacking of CYP2D6 had higher exposure (AUC) to harmaline

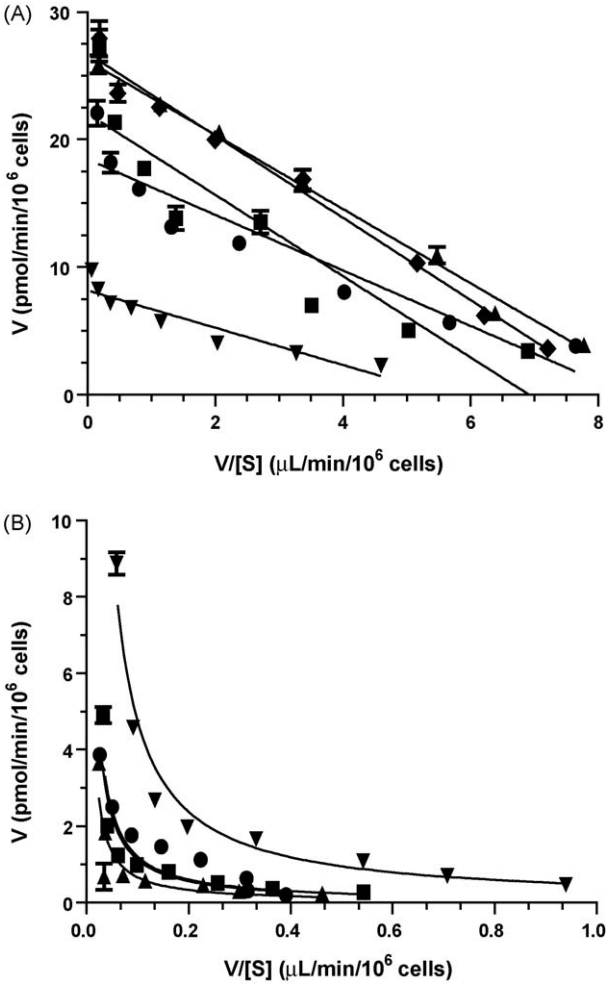

Fig. 2. Eadie–Hofstee plots of harmalol formation from harmaline in human CYP2D6 EM (A) and PM (B) hepatocytes. Values for individual hepatocyte samples represent mean ± SEM of triplicate experiments. CYP2D6 EM hepatocytes ($N = 5$) exhibit monophasic kinetics, whereas PM hepatocytes ($N = 4$) show biphasic kinetics.

(Table 3). For example, AUC values were about 2-fold higher in wild-type mice than Tg-*CYP2D6* mice dosed i.p. with harmaline. Consistently, the elimination of harmaline was slower in wild-type mice, as indicated by a lower systemic clearance (CL) and longer half-life ($T_{1/2}$) (Table 3). Additionally, wild-type mice had

Table 1
Enzyme kinetic parameters estimated for harmalol formation from harmaline in human hepatocytes. CYP2D6 EM and PM hepatocyte data were fit to one-enzyme and two-enzyme Michaelis-Menten equation, respectively. Values for each hepatocyte sample are mean ± SEM from triplicate experiments. CL_{int} (V_{max}/K_m) values were corrected with cell variability. The total CL_{int} values (mean ± SD) in CYP2D6 PM hepatocytes are significantly ($P < 0.001$) lower than those in CYP2D6 EM hepatocytes.

EM	K_m (μM)	V_{max} (pmol/min/10^6 cells)	CL_{int} (μL/min/10^6 cells)
1	3.46 ± 0.47	20.2 ± 0.7	5.84
2	5.99 ± 0.93	25.5 ± 1.1	4.26
3	2.83 ± 0.15	26.1 ± 0.3	9.22
4	2.19 ± 0.29	8.77 ± 0.26	4.00
5	3.24 ± 0.28	26.8 ± 0.6	8.27
Mean	3.54	21.5	6.32
SD	1.45	7.6	2.35

PM	$K_{m\ (1)}$ (μM)	$V_{max\ (1)}$ (pmol/min/10^6 cells)	$CL_{int\ (1)}$ (μL/min/10^6 cells)	$K_{m\ (2)}$ (μM)	$V_{max\ (2)}$ (pmol/min/10^6 cells)	$CL_{int\ (2)}$ (μL/min/10^6 cells)	Total CL_{int} (μL/min/10^6 cells)
1	3.90 ± 0.70	1.73 ± 0.18	0.44	438 ± 355	8.57 ± 4.64	0.020	0.46
2	0.97 ± 0.45	0.72 ± 0.07	0.74		Not saturated		0.74
3	0.27 ± 0.56	0.37 ± 0.15	0.29	400 ± 348	12.1 ± 7.4	0.030	0.32
4	1.21 ± 0.44	1.50 ± 0.21	1.24	354 ± 129	24.8 ± 5.9	0.070	1.31
Mean	1.84	1.08	0.68	397	15.2	0.040	0.71
SD	1.38	0.64	0.42	42.1	8.54	0.027	0.44

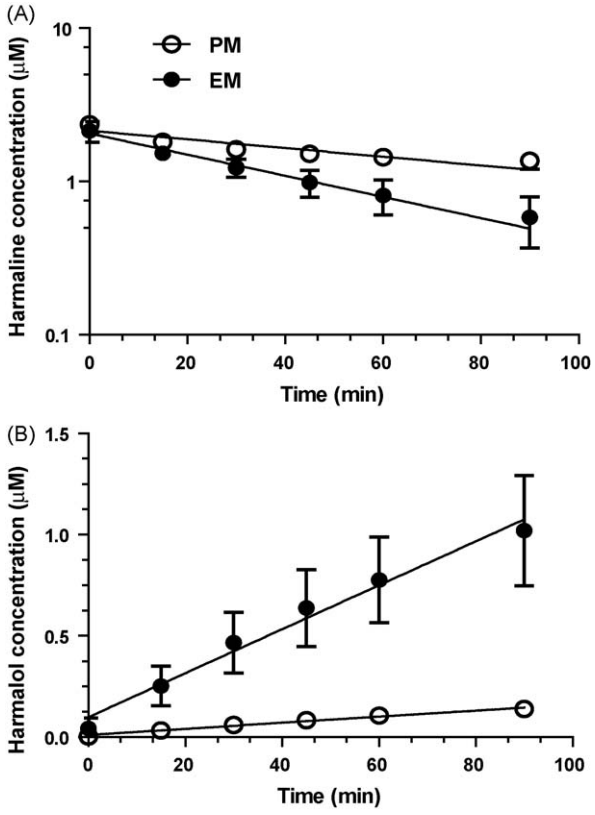

Fig. 3. Harmaline depletion (A) and harmalol production (B) in human CYP2D6 EM ($N = 6$) and PM ($N = 4$) hepatocytes. Values represent mean ± SD. Significant difference in both harmaline depletion and harmalol production is shown for the variations of incubation time and *CYP2D6* genotype/phenotype ($P < 0.0001$; two-way ANOVA).

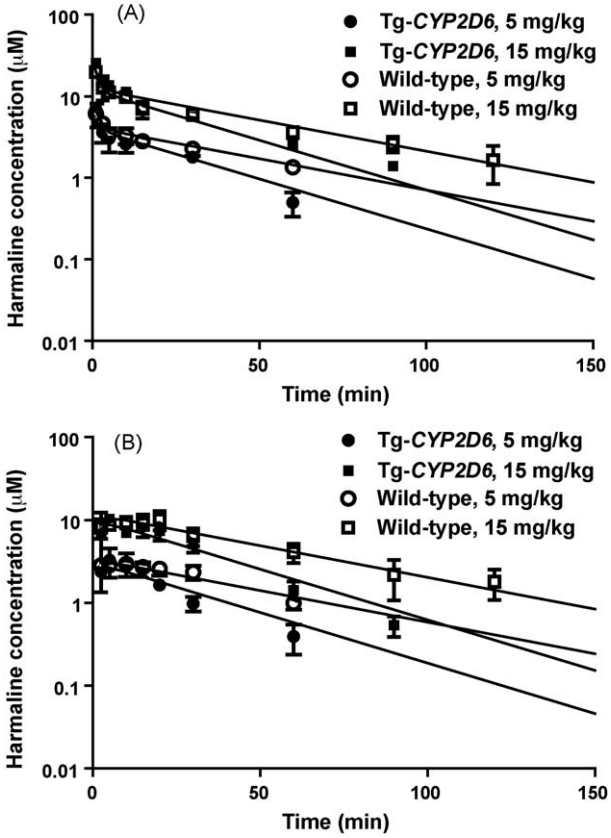

Fig. 4. Serum harmaline concentration versus time curves in wild-type and Tg-*CYP2D6* mice administered i.v. (A) or i.p. (B) with harmaline (5 and 15 mg/kg). Values represent mean ± SD ($N = 3$ at each time point). For each dose, significant difference in harmaline concentrations is shown for the variations of *CYP2D6* genotype and time ($P < 0.05$; two-way ANOVA).

significantly lower blood metabolite (harmalol) concentrations than Tg-*CYP2D6* mice (data not shown), indicating the difference in harmaline *O*-demethylation capacity between the two genotyped mice in vivo. The results suggest that transgenic mice expressing functional CYP2D6 have enhanced capacity to eliminate harmaline, leading to lower and shorter exposure to the drug.

3.4. Pharmacogenetics-based pharmacokinetic model provides mechanistic understanding of the difference in harmaline pharmacokinetics between wild-type and Tg-CYP2D6 mice

Because Tg-*CYP2D6* and wild-type mice differ only in CYP2D6-mediated drug metabolism [1,29,33], we further built a new pharmacogenetics mechanism-based compartmental PK model (Fig. 1) to elucidate harmaline PK difference between the two groups of mice. The mechanistic difference in drug clearance between Tg-*CYP2D6* and wild-type mice (or human CYP2D6 EM and PM subjects) is that the drug is eliminated via CL_{CYP2D6} and CL_{other} in Tg-*CYP2D6* mice, whereas only via CL_{other} in wild-type mice. This model nicely described harmaline PK data in the two genotyped mice, and the results indicated that harmaline clearance by CL_{CYP2D6} and CL_{other} was 60.8 and 96.2 mL/min/kg, respectively (Table 4). In turn, this pharmacogenetics-based PK model can be applied to understand potential difference in PK of

Table 2
Kinetic parameters estimated for harmaline depletion in CYP2D6 PM and EM hepatocytes. Values for individual hepatocytes represent mean of duplicated experiments. Kinetic parameters were estimated with mono-exponential decay model. In vitro CL_{int} value was normalized with cell variability. The in vitro k, $T_{1/2}$ and CL_{int} values (mean ± SD) are all significantly ($P < 0.01$) different between CYP2D6 EM and PM hepatocytes.

CYP2D6 status	Hepatocyte	k ($\times 10^{-3}$ min^{-1})	In vitro $T_{1/2}$ (min)	In vitro CL_{int} (μL/min/10^6 cells)
PM	1	7.80	88.9	34.7
	2	8.24	84.2	32.7
	3	5.24	132	23.9
	4	5.04	138	22.5
	Mean	6.58	111	28.5
	SD	1.67	28	6.2
EM	1	18.4	37.6	79.9
	2	24.9	27.9	102
	3	18.2	38.2	84.0
	4	10.0	69.0	42.4
	5	11.2	61.8	46.2
	6	16.5	42.0	71.7
	Mean	16.5	46.1	71.1
	SD	5.4	15.8	23.1

Table 3
Pharmacokinetic parameters (mean ± SD) of harmaline determined by non-compartmental analysis using WinNonLin.

Parameters	Units	Tg-*CYP2D6*				Wild-type			
		i.v. 5 mg/kg	i.v. 15 mg/kg	i.p. 5 mg/kg	i.p. 15 mg/kg	i.v. 5 mg/kg	i.v. 15 mg/kg	i.p. 5 mg/kg	i.p. 15 mg/kg
$AUC_{0\rightarrow\infty}$	Min μmol/L	134 ± 19	544 ± 10	94.3 ± 9.5	359 ± 15	233 ± 34*	682 ± 114	175 ± 28**	662 ± 39***
CL	mL/min/kg	176 ± 27	128 ± 2	–	–	102 ± 16*	104 ± 16	–	–
V_{ss}	L/kg	4.41 ± 0.08	5.14 ± 0.46	–	–	5.74 ± 1.02	6.23 ± 0.57	–	–
T_{max}	Min	–	–	6.67 ± 2.89	8.33 ± 5.77	–	–	5.83 ± 3.82	15.0 ± 5.0
C_{max}	μmol/L	–	–	3.82 ± 1.04	11.0 ± 1.0	–	–	3.02 ± 0.25	11.5 ± 1.3
$T_{1/2}$	Min	18.0 ± 2.9	36.5 ± 3.3	17.8 ± 2.7	19.1 ± 3.5	41.9 ± 11.7*	43.1 ± 9.6	32.3 ± 10.7	35.5 ± 5.1*
F	%	–	–	68.6 ± 16.6	60.0 ± 2.4	–	–	73.7 ± 20.5	98.2 ± 10.1

* $P < 0.05$ compared with the corresponding values in Tg-*CYP2D6* mice receiving the same treatment.
** $P < 0.01$ compared with the corresponding values in Tg-*CYP2D6* mice receiving the same treatment.
*** $P < 0.001$ compared with the corresponding values in Tg-*CYP2D6* mice receiving the same treatment.

CYP2D6-metabolized drugs between human CYP2D6 PM and EM subjects.

3.5. High dose of harmaline induces more severe hypothermia in wild-type mice than Tg-CYP2D6 mice

To investigate if the difference in harmaline PK could be translated into significant difference in drug response, we compared harmaline-induced hypothermic effects between wild-type and Tg-*CYP2D6* mice. Administration of harmaline resulted in a rapid decrease in body temperature in both wild-type and Tg-*CYP2D6* mice (Fig. 5), whereas injection of drug vehicle had no significant effects within the period (data not shown). Importantly, the hypothermia induced by 15 mg/kg of harmaline was more severe in wild-type mice than Tg-*CYP2D6* mice. In particular, wild-type mice recovered from hypothermia at a lower rate, which was associated with lower drug clearance and higher exposure to harmaline (Fig. 4 and Table 3). The body temperature data were fit to the indirect response PD model with stimulation of k_{out} (IDRIV), which possibly involves the serotonergic action of harmaline [30]. As expected, there was no difference in PD parameters (Table 5) estimated for the two genotyped mice, suggesting that the observed difference in hypothermia was caused by the differences in harmaline PK between wild-type and Tg-*CYP2D6* mice.

3.6. Harmaline inhibits marble-burying behavior to a greater degree in wild-type mice than Tg-CYP2D6 mice

In addition, we employed marble-burying test [34–36] to evaluate the difference in harmaline drug effects between wild-type and Tg-*CYP2D6* mice. Of note, the behavior of burying harmless marbles by mice is considered as an animal model of obsessive–compulsive disorder, and may indicate the anxiolytic activity of a drug. The results showed that Tg-*CYP2D6* mice dosed i.p. with 5.0 or 7.5 mg/kg of harmaline buried a significantly greater number of marbles than wild-type mice treated with the same dose of harmaline (Fig. 6). Overall, harmaline dose responses in the two genotyped mice were significantly different. Particularly, wild-type mice had a significantly lower ED_{50} value (5.00 ± 1.04 mg/kg) and a steeper Hill slope (−5.79 ± 1.58) than Tg-*CYP2D6* mice (ED_{50} 6.75 ± 1.05 mg/kg and Hill slope −4.28 ± 0.84,

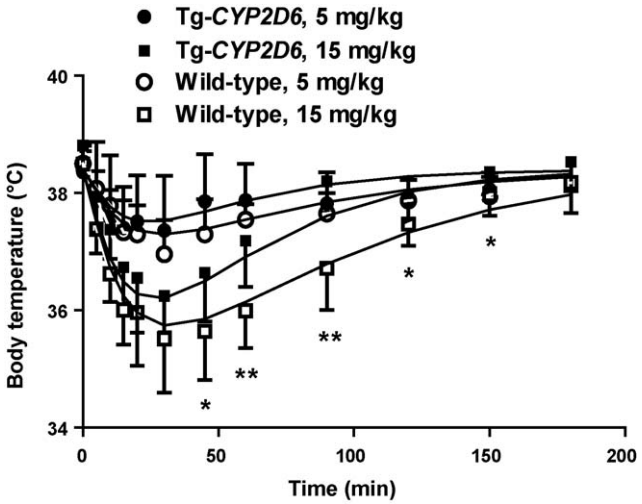

Fig. 5. Hypothermic effects induced by harmaline (5 and 15 mg/kg, i.p.) in wild-type and Tg-*CYP2D6* mice. Values represent mean ± SD ($N = 8$ in each group). For the high dose (15 mg/kg), significant difference is shown for the variations of *CYP2D6* genotype and time ($P < 0.001$; two-way ANOVA). Difference (*$P < 0.05$, **$P < 0.01$) is also noted between the two genotyped mice treated with 15 mg/kg harmaline at specific time points.

Table 4
Pharmacokinetic parameters of harmaline in Tg-*CYP2D6* and wild-type mice estimated by the pharmacogenetic-based compartmental analysis. CL_{CYP2D6}, clearance contributed by CYP2D6-mediated metabolism; CL_{other}, clearance contributed by other elimination pathways; CL_D, distribution clearance between central and peripheral compartments; V_C, volume of distribution of the central compartment; V_T, volume of distribution of the peripheral compartment; K_a, absorption rate constant; *F* represents the bioavailability of certain dose of drug administered to different mouse models.

Parameter	Unit	Estimated value (CV%)
K_a	1/min	0.307 (14.9)
V_C	L/kg	2.43 (12.1)
V_T	L/kg	2.86 (10.1)
CL_D	mL/min/kg	879 (25.3)
CL_{CYP2D6}	mL/min/kg	60.8 (27.6)
CL_{other}	mL/min/kg	96.2 (8.68)
$F_{CYP2D6,\ 5\ mg/kg}$	%	68.8 (19.5)
$F_{CYP2D6,\ 15\ mg/kg}$	%	80.1 (7.32)
$F_{WT,\ 5\ mg/kg}$	%	74.2 (15.8)
$F_{WT,\ 15\ mg/kg}$	%	90.3 (6.08)

Table 5
Estimated pharmacodynamic parameters describing harmaline-induced hypothermic effects in Tg-*CYP2D6* and wild-type mice. T_0, the initial condition of body temperature; k_{out}, the first order rate constant associated with the cooling of the body; S_{max}, the maximum stimulus harmaline can produce; SC_{50}, drug concentration required to produce 50% of the maximum stimulus.

	Tg-*CYP2D6*	Wild-type
Parameter	Estimate (CV%)	Estimate (CV%)
T_0 (°C)	38.4 (0.28)	38.4 (0.20)
k_{out} (1/h)	0.0671 (26.0)	0.0713 (9.79)
S_{max}	0.180 (71.3)	0.210 (19.3)
SC_{50} (μM)	11.8 (101)	10.7 (31.7)

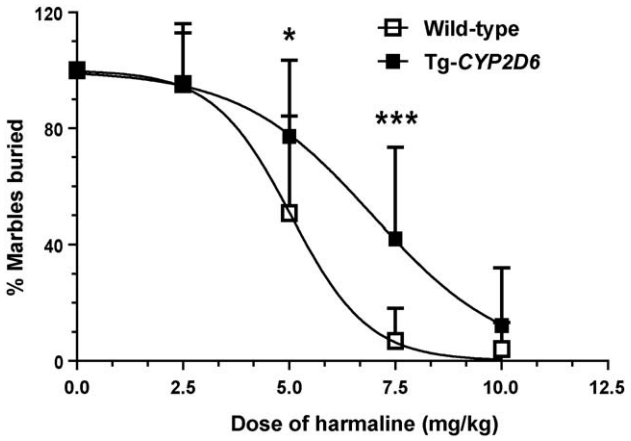

Fig. 6. Marble-burying behavior of wild-type and Tg-*CYP2D6* mice exposed to harmaline (0–10 mg/kg, i.p.). Values represent mean ± SD ($N = 14$ in each group). The dose responses are significantly different between the two genotyped mice ($P < 0.001$; two-way ANOVA). Difference ($^{*}P < 0.05$, $^{***}P < 0.001$) is also noted between the two genotyped mice at specific doses. It is notable that wild-type mice exhibit a significantly lower ED_{50} value (5.00 ± 1.04 mg/kg) and steeper Hill slope (−5.79 ± 1.58) than Tg-*CYP2D6* mice (6.75 ± 1.05 mg/kg and −4.28 ± 0.84, respectively).

respectively). These findings suggest that wild-type mice lacking of CYP2D6 are more sensitive to harmaline.

4. Discussion

Humans are exposed to endogenously synthesized, dietary or recreational β-carbolines, an important group of indoleamines that have a wide spectrum of biochemical, pharmacological and toxicological properties. Harmaline represents a β-carboline alkaloid that shows both neurotoxic and neuroprotective effects, and cases of harmaline-related intoxication have been documented in recent years [23–25]. Our previous study has revealed an important contribution of polymorphic CYP2D6 to harmaline *O*-demethylation metabolism [28], which is the predominant pathway in harmaline clearance in rat models [27]. The data from current study, using human hepatocytes and transgenic mouse models, clearly demonstrated that CYP2D6 status had significant impact on harmaline total clearance and drug responses, suggesting that CYP2D6 polymorphism could be an additional risk factor in harmaline intoxication.

CYP2D6 genetic polymorphism is an important factor causing inter-patient variations in PK, and is well recognized for its clinical significance [2]. Defect of *CYP2D6* gene accurately predicts CYP2D6 PM phenotype, in comparison to EM carrying functional CYP2D6 alleles. Of note, 7–10% of Caucasians are CYP2D6 PMs who, taking standard or higher dose of CYP2D6-inactivated drug, may have higher blood drug concentrations. While harmaline is mainly eliminated via *O*-demethylation metabolism [27] and CYP2D6 significantly contributes to this biotransformation [28], CYP2D6 deficiency led to the impaired harmaline *O*-demethylase capacity (Fig. 2 and Table 1) and slower substrate depletion (Fig. 3 and Table 2). The less dramatic difference in substrate depletion (2.5-fold) than metabolite formation (9-fold) between EM and PM hepatocytes may reflect the actual contribution of CYP2D6-mediated metabolism to total harmaline depletion. In comparison to Tg-*CYP2D6* mice, wild-type mice lacking of CYP2D6 activity indeed had higher and longer exposure to harmaline (Fig. 4 and Table 3). Note that the Tg-*CYP2D6* and wild-type mice may be valuable animal models for human CYP2D6 EMs and PMs, respectively [29,33], in assessing the significance of CYP2D6-mediated drug metabolism at the systemic level. Our findings suggest that CYP2D6 PMs would have lower harmaline hepatic clearance, leading to potential risk of higher exposure to the drug. It is also documented that people taking harmine, another β-carboline substance metabolized by CYP2D6, CYP1A and CYP2C [28], show distinct slow and fast metabolizer phenotypes [37]. Together, the presence of metabolic pharmacogenetics may raise additional concerns for use of these psychotropic β-carboline xenobiotics.

Assessing the risk of polymorphic metabolism for a drug is important not only in clinical pharmacotherapy but also in drug discovery and development. A quantitative relationship between in vitro CYP2D6 metabolism and in vivo PK has been constructed for evaluation of the impact of CYP2D6 polymorphic metabolism [38]. The pharmacogenetics-based compartmental PK model (Fig. 1) described in current study was developed from the two genotyped animal models that differ in CYP2D6 drug-metabolizing activity [29,33]. This model may be readily applied to human subjects (e.g., PMs and EMs) with different metabolic capacity caused by polymorphic drug-metabolizing enzyme. When linear drug clearance is assumed, the function of AUC ratio between PMs and EMs ($R_{AUC} = AUC^{PM}/AUC^{EM} = 1 + CL_{CYP2D6}/CL_{other}$) derived from our model (Fig. 1) is essentially the same as that ($R_{AUC} = 1/(1 - fm_{CYP2D6})$) in Gibbs model [38], in which fm_{CYP2D6}, the fraction of drug clearance by CYP2D6 enzyme, equals to CL_{CYP2D6} divided by the sum of CL_{CYP2D6} and CL_{other}. One may notice that fm_{CYP2D6} determined by in vitro assays with human liver microsomes or hepatocytes [38] is rather a fraction of hepatic clearance than total clearance. Therefore, use of in vitro fm_{CYP2D6} value, which overlooks renal or other drug clearance mechanisms, might provide an overestimation of the actual in vivo fm_{CYP2D6} and an exaggerated prediction of the impact of polymorphic metabolism on PK. Meanwhile, quantitative prediction of human PK from transgenic mouse data remains a challenge [33] unless reliable mouse-to-human scaling factors exist for drug clearance [39]. Nevertheless, clinical studies are indispensable to gain a clear understanding of the impact of polymorphic metabolism on drug exposure, and our PK model (Fig. 1) may provide a helpful insight.

It is noteworthy that significant difference in PK may not be translated into considerable difference in PD, due to distinct PD relationship (e.g., the absence of linear dose-effect relationship) [40] and sensitivity of the assay for drug response. Harmaline is able to induce a variety of biochemical, physiological and pharmacological effects. Current study investigated the change of mouse body temperature and marble-burying behavior following the administration of harmaline. Although exposure to 5 mg/kg i.p. harmaline was significantly higher in wild-type mice than Tg-*CYP2D6* mice (Table 3), the change of body temperature was not significantly different between the two genotyped mice (Fig. 5). In contrast, the anxiolytic activity of 5 mg/kg i.p. harmaline shown in mouse marble-burying test was significantly higher in wild-type mice (Fig. 6). Furthermore, wild-type mice exposed to15 mg/kg of harmaline showed more severe hypothermia than transgenic mice (Fig. 5), which is consistent with drug exposure data (Fig. 3 and Table 3). These findings suggest that PK/PD relationship need be understood for precise assessment of polymorphic metabolism on drug responses.

In summary, CYP2D6 drug-metabolizing enzyme plays an important role in harmaline clearance. Compared to human CYP2D6 EM hepatocytes, PM hepatocytes showed defective harmaline *O*-demethylase capacity, leading to lower rate of substrate depletion. Compared to Tg-*CYP2D6* mice, wild-type mice had significantly higher and longer exposure to harmaline xenobiotics, which was translated into more severe hypothermia and greater extent change in marble-burying behavior. Our findings suggest that distinct CYP2D6 status can cause considerable variations in harmaline metabolism, PK and PD, and CYP2D6 deficiency may lead to increased risk when high dose of harmaline

is used. In addition, the pharmacogenetics-based PK model can be generalized to understand and assess the degree of PK difference caused by other polymorphic drug-metabolizing enzyme in different populations.

Acknowledgements

The project was supported by Award Number R01DA021172 from the National Institute On Drug Abuse (NIDA), National Institutes of Health (NIH). The authors also thank the Pharmaceutical Sciences Instrumentation Facility at University at Buffalo for use of LC-MS system that was obtained with Shared Instrumentation Grants S10RR014592 from the National Center for Research Resources, NIH.

References

[1] Yu AM, Idle JR, Gonzalez FJ. Polymorphic cytochrome P450 2D6: humanized mouse model and endogenous substrates. Drug Metab Rev 2004;36(2):243–77.
[2] Zanger UM, Raimundo S, Eichelbaum M. Cytochrome P450 2D6: overview and update on pharmacology, genetics, biochemistry. Naunyn Schmiedebergs Arch Pharmacol 2004;369(1):23–37.
[3] Sellers EM, Tyndale RF. Mimicking gene defects to treat drug dependence. Ann N Y Acad Sci 2000;909:233–46.
[4] Maurer HH, Kraemer T, Springer D, Staack RF. Chemistry, pharmacology, toxicology, and hepatic metabolism of designer drugs of the amphetamine (ecstasy), piperazine, and pyrrolidinophenone types: a synopsis. Ther Drug Monit 2004;26(2):127–31.
[5] Theobald DS, Maurer HH. Identification of monoamine oxidase and cytochrome P450 isoenzymes involved in the deamination of phenethylamine-derived designer drugs (2C-series). Biochem Pharmacol 2007;73(2):287–97.
[6] Ramamoorthy Y, Yu AM, Suh N, Haining RL, Tyndale RF, Sellers EM. Reduced (±)-3,4-methylenedioxymethamphetamine (“Ecstasy”) metabolism with cytochrome P450 2D6 inhibitors and pharmacogenetic variants in vitro. Biochem Pharmacol 2002;63(12):2111–9.
[7] Yu AM. Indolealkylamines: biotransformations and potential drug-drug interactions. Aaps J 2008;10(2):242–53.
[8] Narimatsu S, Yonemoto R, Saito K, Takaya K, Kumamoto T, Ishikawa T, et al. Oxidative metabolism of 5-methoxy-*N*,*N*-diisopropyltryptamine (Foxy) by human liver microsomes and recombinant cytochrome P450 enzymes. Biochem Pharmacol 2006;71(9):1377–85.
[9] Narimatsu S, Yonemoto R, Masuda K, Katsu T, Asanuma M, Kamata T, et al. Oxidation of 5-methoxy-*N*,*N*-diisopropyltryptamine in rat liver microsomes and recombinant cytochrome P450 enzymes. Biochem Pharmacol 2008;75(3):752–60.
[10] Sauer C, Peters FT, Schwaninger AE, Meyer MR, Maurer HH. Investigations on the cytochrome P450 (CYP) isoenzymes involved in the metabolism of the designer drugs *N*-(1-phenyl cyclohexyl)-2-ethoxyethanamine and *N*-(1-phenylcyclohexyl)-2-methoxyethanamine. Biochem Pharmacol 2009;77(3):444–50.
[11] Staack RF, Paul LD, Springer D, Kraemer T, Maurer HH. Cytochrome P450 dependent metabolism of the new designer drug 1-(3-trifluoromethylphenyl)piperazine (TFMPP), In vivo studies in Wistar and Dark Agouti rats as well as in vitro studies in human liver microsomes. Biochem Pharmacol 2004;67(2):235–44.
[12] Rutter JL. Symbiotic relationship of pharmacogenetics and drugs of abuse. Aaps J 2006;8(1):E174–84.
[13] Lamchouri F, Settaf A, Cherrah Y, El Hamidi M, Tligui N, Lyoussi B, et al. Experimental toxicity of *Peganum harmala* seeds. Ann Pharm Fr 2002;60(2):123–9.
[14] McKenna DJ. Clinical investigations of the therapeutic potential of ayahuasca: rationale and regulatory challenges. Pharmacol Ther 2004;102(2):111–29.
[15] Lee CS, Han ES, Jang YY, Han JH, Ha HW, Kim DE. Protective effect of harmalol and harmaline on MPTP neurotoxicity in the mouse and dopamine-induced damage of brain mitochondria and PC12 cells. J Neurochem 2000;75(2):521–31.
[16] Moura DJ, Richter MF, Boeira JM, Pegas Henriques JA, Saffi J. Antioxidant properties of beta-carboline alkaloids are related to their antimutagenic and antigenotoxic activities. Mutagenesis 2007;22(4):293–302.
[17] Hilber P, Chapillon P. Effects of harmaline on anxiety-related behavior in mice. Physiol Behav 2005;86(1–2):164–7.
[18] Berrougui H, Martin-Cordero C, Khalil A, Hmamouchi M, Ettaib A, Marhuenda E, et al. Vasorelaxant effects of harmine and harmaline extracted from *Peganum harmala* L. seeds in isolated rat aorta. Pharmacol Res 2006;54(2):150–7.
[19] Monsef HR, Ghobadi A, Iranshahi M, Abdollahi M. Antinociceptive effects of *Peganum harmala* L. alkaloid extract on mouse formalin test. J Pharm Pharm Sci 2004;7(1):65–9.
[20] Miwa H. Rodent models of tremor. Cerebellum 2007;6(1):66–72.
[21] Martin FC, Thu Le A, Handforth A. Harmaline-induced tremor as a potential preclinical screening method for essential tremor medications. Mov Disord 2005;20(3):298–305.
[22] Wilms H, Sievers J, Deuschl G. Animal models of tremor. Mov Disord 1999;14(4):557–71.
[23] Frison G, Favretto D, Zancanaro F, Fazzin G, Ferrara SD. A case of beta-carboline alkaloid intoxication following ingestion of *Peganum harmala* seed extract. Forensic Sci Int 2008;179(2–3):e37–43.
[24] Brush DE, Bird SB, Boyer EW. Monoamine oxidase inhibitor poisoning resulting from Internet misinformation on illicit substances. J Toxicol Clin Toxicol 2004;42(2):191–5.
[25] Sklerov J, Levine B, Moore KA, King T, Fowler D. A fatal intoxication following the ingestion of 5-methoxy-*N*,*N*-dimethyltryptamine in an ayahuasca preparation. J Anal Toxicol 2005;29(8):838–41.
[26] Lorenz D, Deuschl G. Update on pathogenesis and treatment of essential tremor. Curr Opin Neurol 2007;20(4):447–52.
[27] Ho BT, Estevez V, Fritchie GE, Tansey LW, Idanpaan-Heikkila J, McIsaac WM. Metabolism of harmaline in rats. Biochem Pharmacol 1971;20(6):1313–9.
[28] Yu AM, Idle JR, Krausz KW, Kupfer A, Gonzalez FJ. Contribution of individual cytochrome P450 isozymes to the *O*-demethylation of the psychotropic beta-carboline alkaloids harmaline and harmine. J Pharmacol Exp Ther 2003;305(1):315–22.
[29] Corchero J, Granvil CP, Akiyama TE, Hayhurst GP, Pimprale S, Feigenbaum L, et al. The CYP2D6 humanized mouse: effect of the human CYP2D6 transgene and HNF4alpha on the disposition of debrisoquine in the mouse. Mol Pharmacol 2001;60(6):1260–7.
[30] Abdel-Fattah AF, Matsumoto K, Gammaz HA, Watanabe H. Hypothermic effect of harmala alkaloid in rats: involvement of serotonergic mechanism. Pharmacol Biochem Behav 1995;52(2):421–6.
[31] Granvil CP, Yu AM, Elizondo G, Akiyama TE, Cheung C, Feigenbaum L, et al. Expression of the human CYP3A4 gene in the small intestine of transgenic mice: in vitro metabolism and pharmacokinetics of midazolam. Drug Metab Dispos 2003;31(5):548–58.
[32] Dayneka NL, Garg V, Jusko WJ. Comparison of four basic models of indirect pharmacodynamic responses. J Pharmacokinet Biopharm 1993;21(4):457–78.
[33] Gonzalez FJ, Yu AM. Cytochrome P450 and xenobiotic receptor humanized mice. Annu Rev Pharmacol Toxicol 2006;46:41–64.
[34] Njung'e K, Handley SL. Evaluation of marble-burying behavior as a model of anxiety. Pharmacol Biochem Behav 1991;38(1):63–7.
[35] Borsini F, Podhorna J, Marazziti D. Do animal models of anxiety predict anxiolytic-like effects of antidepressants? Psychopharmacology (Berl) 2002;163(2):121–41.
[36] Cryan JF, Holmes A. The ascent of mouse: advances in modelling human depression and anxiety. Nat Rev Drug Discov 2005;4(9):775–90.
[37] Callaway JC. Fast and slow metabolizers of Hoasca. J Psychoactive Drugs 2005;37(2):157–61.
[38] Gibbs JP, Hyland R, Youdim K. Minimizing polymorphic metabolism in drug discovery: evaluation of the utility of in vitro methods for predicting pharmacokinetic consequences associated with CYP2D6 metabolism. Drug Metab Dispos 2006;34(9):1516–22.
[39] Tang H, Hussain A, Leal M, Mayersohn M, Fluhler E. Interspecies prediction of human drug clearance based on scaling data from one or two animal species. Drug Metab Dispos 2007;35(10):1886–93.
[40] Kirchheiner J, Fuhr U, Brockmoller J. Pharmacogenetics-based therapeutic recommendations—ready for clinical practice? Nat Rev Drug Discov 2005;4(8):639–47.